

# **W pair production cross-section and W branching fractions in $e^+e^-$ interactions at 183 GeV**

DELPHI Collaboration

## **Abstract**

The cross-section for the process  $e^+e^- \rightarrow W^+W^-$  has been measured with the data sample collected by DELPHI at an average centre-of-mass energy of 182.65 GeV and corresponding to an integrated luminosity of  $53 \text{ pb}^{-1}$ . Based on the 770 events selected as  $WW$  candidates, the cross-section for the doubly resonant process  $\sigma(e^+e^- \rightarrow W^+W^-) = 15.86 \pm 0.69 \text{ (stat)} \pm 0.26 \text{ (syst)} \text{ pb}$  has been measured and found to be in good agreement with the Standard Model expectation. The branching fractions of the  $W$  decay were also measured. From these a value of the CKM mixing matrix element  $|V_{cs}| = 0.985 \pm 0.073 \text{ (stat)} \pm 0.025 \text{ (syst)}$  was derived. Our previously published  $WW$  cross-section measurements and the derived measurement of  $m_W$  have been revised and updated with the present cross-section measurement to yield  $m_W = 80.49 \pm 0.43 \text{ (stat)} \pm 0.09 \text{ (syst)} \pm 0.03 \text{ (LEP)} \text{ GeV}/c^2$ .

(Accepted by Physics Letters B)



L.Tortora<sup>38</sup>, G.Transtomer<sup>24</sup>, D.Treille<sup>9</sup>, G.Tristram<sup>8</sup>, M.Trochimczuk<sup>51</sup>, C.Troncon<sup>27</sup>, A.Tsirou<sup>9</sup>, M-L.Turluer<sup>39</sup>, I.A.Tyapkin<sup>16</sup>, S.Tzamarias<sup>11</sup>, O.Ullaland<sup>9</sup>, V.Uvarov<sup>42</sup>, G.Valenti<sup>5</sup>, E.Vallazza<sup>46</sup>, G.W.Van Apeldoorn<sup>30</sup>, P.Van Dam<sup>30</sup>, W.K.Van Doninck<sup>2</sup>, J.Van Eldik<sup>30</sup>, A.Van Lysebetten<sup>2</sup>, I.Van Vulpen<sup>30</sup>, N.Vassilopoulos<sup>34</sup>, G.Vegni<sup>27</sup>, L.Ventura<sup>35</sup>, W.Venus<sup>36,9</sup>, F.Verbeure<sup>2</sup>, M.Verlato<sup>35</sup>, L.S.Vertogradov<sup>16</sup>, V.Verzi<sup>37</sup>, D.Vilanova<sup>39</sup>, L.Vitale<sup>46</sup>, E.Vlasov<sup>42</sup>, A.S.Vodopyanov<sup>16</sup>, C.Vollmer<sup>17</sup>, G.Voulgaris<sup>3</sup>, V.Vrba<sup>12</sup>, H.Wahlen<sup>52</sup>, C.Walck<sup>44</sup>, C.Weiser<sup>17</sup>, D.Wicke<sup>52</sup>, J.H.Wickens<sup>2</sup>, G.R.Wilkinson<sup>9</sup>, M.Winter<sup>10</sup>, M.Witek<sup>18</sup>, G.Wolf<sup>9</sup>, J.Yi<sup>1</sup>, O.Yushchenko<sup>42</sup>, A.Zaitsev<sup>42</sup>, A.Zalewska<sup>18</sup>, P.Zalewski<sup>51</sup>, D.Zavrtanik<sup>43</sup>, E.Zevgolatakos<sup>11</sup>, N.I.Zimin<sup>16,24</sup>, G.C.Zucchelli<sup>44</sup>, G.Zumerle<sup>35</sup>

---

<sup>1</sup>Department of Physics and Astronomy, Iowa State University, Ames IA 50011-3160, USA

<sup>2</sup>Physics Department, Univ. Instelling Antwerpen, Universiteitsplein 1, BE-2610 Wilrijk, Belgium and IIHE, ULB-VUB, Pleinlaan 2, BE-1050 Brussels, Belgium

and Faculté des Sciences, Univ. de l'Etat Mons, Av. Maistriau 19, BE-7000 Mons, Belgium

<sup>3</sup>Physics Laboratory, University of Athens, Solonos Str. 104, GR-10680 Athens, Greece

<sup>4</sup>Department of Physics, University of Bergen, Allégaten 55, NO-5007 Bergen, Norway

<sup>5</sup>Dipartimento di Fisica, Università di Bologna and INFN, Via Irnerio 46, IT-40126 Bologna, Italy

<sup>6</sup>Centro Brasileiro de Pesquisas Físicas, rua Xavier Sigaud 150, BR-22290 Rio de Janeiro, Brazil

and Depto. de Física, Pont. Univ. Católica, C.P. 38071 BR-22453 Rio de Janeiro, Brazil

and Inst. de Física, Univ. Estadual do Rio de Janeiro, rua São Francisco Xavier 524, Rio de Janeiro, Brazil

<sup>7</sup>Comenius University, Faculty of Mathematics and Physics, Mlynska Dolina, SK-84215 Bratislava, Slovakia

<sup>8</sup>Collège de France, Lab. de Physique Corpusculaire, IN2P3-CNRS, FR-75231 Paris Cedex 05, France

<sup>9</sup>CERN, CH-1211 Geneva 23, Switzerland

<sup>10</sup>Institut de Recherches Subatomiques, IN2P3 - CNRS/ULP - BP20, FR-67037 Strasbourg Cedex, France

<sup>11</sup>Institute of Nuclear Physics, N.C.S.R. Demokritos, P.O. Box 60228, GR-15310 Athens, Greece

<sup>12</sup>FZU, Inst. of Phys. of the C.A.S. High Energy Physics Division, Na Slovance 2, CZ-180 40, Praha 8, Czech Republic

<sup>13</sup>Dipartimento di Fisica, Università di Genova and INFN, Via Dodecaneso 33, IT-16146 Genova, Italy

<sup>14</sup>Institut des Sciences Nucléaires, IN2P3-CNRS, Université de Grenoble 1, FR-38026 Grenoble Cedex, France

<sup>15</sup>Helsinki Institute of Physics, HIP, P.O. Box 9, FI-00014 Helsinki, Finland

<sup>16</sup>Joint Institute for Nuclear Research, Dubna, Head Post Office, P.O. Box 79, RU-101 000 Moscow, Russian Federation

<sup>17</sup>Institut für Experimentelle Kernphysik, Universität Karlsruhe, Postfach 6980, DE-76128 Karlsruhe, Germany

<sup>18</sup>Institute of Nuclear Physics and University of Mining and Metallurgy, Ul. Kawiora 26a, PL-30055 Krakow, Poland

<sup>19</sup>Université de Paris-Sud, Lab. de l'Accélérateur Linéaire, IN2P3-CNRS, Bât. 200, FR-91405 Orsay Cedex, France

<sup>20</sup>School of Physics and Chemistry, University of Lancaster, Lancaster LA1 4YB, UK

<sup>21</sup>LIP, IST, FCUL - Av. Elias Garcia, 14-1<sup>o</sup>, PT-1000 Lisboa Codex, Portugal

<sup>22</sup>Department of Physics, University of Liverpool, P.O. Box 147, Liverpool L69 3BX, UK

<sup>23</sup>LPNHE, IN2P3-CNRS, Univ. Paris VI et VII, Tour 33 (RdC), 4 place Jussieu, FR-75252 Paris Cedex 05, France

<sup>24</sup>Department of Physics, University of Lund, Sölvegatan 14, SE-223 63 Lund, Sweden

<sup>25</sup>Université Claude Bernard de Lyon, IPNL, IN2P3-CNRS, FR-69622 Villeurbanne Cedex, France

<sup>26</sup>Univ. d'Aix - Marseille II - CPP, IN2P3-CNRS, FR-13288 Marseille Cedex 09, France

<sup>27</sup>Dipartimento di Fisica, Università di Milano and INFN, Via Celoria 16, IT-20133 Milan, Italy

<sup>28</sup>Niels Bohr Institute, Blegdamsvej 17, DK-2100 Copenhagen Ø, Denmark

<sup>29</sup>NC, Nuclear Centre of MFF, Charles University, Areal MFF, V Holesovickach 2, CZ-180 00, Praha 8, Czech Republic

<sup>30</sup>NIKHEF, Postbus 41882, NL-1009 DB Amsterdam, The Netherlands

<sup>31</sup>National Technical University, Physics Department, Zografou Campus, GR-15773 Athens, Greece

<sup>32</sup>Physics Department, University of Oslo, Blindern, NO-1000 Oslo 3, Norway

<sup>33</sup>Dpto. Física, Univ. Oviedo, Avda. Calvo Sotelo s/n, ES-33007 Oviedo, Spain

<sup>34</sup>Department of Physics, University of Oxford, Keble Road, Oxford OX1 3RH, UK

<sup>35</sup>Dipartimento di Fisica, Università di Padova and INFN, Via Marzolo 8, IT-35131 Padua, Italy

<sup>36</sup>Rutherford Appleton Laboratory, Chilton, Didcot OX11 0QX, UK

<sup>37</sup>Dipartimento di Fisica, Università di Roma II and INFN, Tor Vergata, IT-00173 Rome, Italy

<sup>38</sup>Dipartimento di Fisica, Università di Roma III and INFN, Via della Vasca Navale 84, IT-00146 Rome, Italy

<sup>39</sup>DAPNIA/Service de Physique des Particules, CEA-Saclay, FR-91191 Gif-sur-Yvette Cedex, France

<sup>40</sup>Instituto de Física de Cantabria (CSIC-UC), Avda. los Castros s/n, ES-39006 Santander, Spain

<sup>41</sup>Dipartimento di Fisica, Università degli Studi di Roma La Sapienza, Piazzale Aldo Moro 2, IT-00185 Rome, Italy

<sup>42</sup>Inst. for High Energy Physics, Serpukov P.O. Box 35, Protvino, (Moscow Region), Russian Federation

<sup>43</sup>J. Stefan Institute, Jamova 39, SI-1000 Ljubljana, Slovenia and Laboratory for Astroparticle Physics,

Nova Gorica Polytechnic, Kostanjevska 16a, SI-5000 Nova Gorica, Slovenia,

and Department of Physics, University of Ljubljana, SI-1000 Ljubljana, Slovenia

<sup>44</sup>Fysikum, Stockholm University, Box 6730, SE-113 85 Stockholm, Sweden

<sup>45</sup>Dipartimento di Fisica Sperimentale, Università di Torino and INFN, Via P. Giuria 1, IT-10125 Turin, Italy

<sup>46</sup>Dipartimento di Fisica, Università di Trieste and INFN, Via A. Valerio 2, IT-34127 Trieste, Italy

and Istituto di Fisica, Università di Udine, IT-33100 Udine, Italy

<sup>47</sup>Univ. Federal do Rio de Janeiro, C.P. 68528 Cidade Univ., Ilha do Fundão BR-21945-970 Rio de Janeiro, Brazil

<sup>48</sup>Department of Radiation Sciences, University of Uppsala, P.O. Box 535, SE-751 21 Uppsala, Sweden

<sup>49</sup>IFIC, Valencia-CSIC, and D.F.A.M.N., U. de Valencia, Avda. Dr. Moliner 50, ES-46100 Burjassot (Valencia), Spain

<sup>50</sup>Institut für Hochenergiephysik, Österr. Akad. d. Wissensch., Nikolsdorfergasse 18, AT-1050 Vienna, Austria

<sup>51</sup>Inst. Nuclear Studies and University of Warsaw, Ul. Hoza 69, PL-00681 Warsaw, Poland

<sup>52</sup>Fachbereich Physik, University of Wuppertal, Postfach 100 127, DE-42097 Wuppertal, Germany

<sup>53</sup>On leave of absence from IHEP Serpukhov

<sup>54</sup>Now at University of Florida

# 1 Introduction

The cross-section for the doubly resonant production of  $W$  bosons has been measured with the data sample collected by DELPHI at the average centre-of-mass energy of  $182.65 \pm 0.06$  GeV. The total integrated luminosity corresponds to  $53 \text{ pb}^{-1}$ ; its systematic error is estimated to be  $\pm 0.6\%$ , which is dominated by the experimental uncertainty of the Bhabha measurements of  $\pm 0.5\%$ . The luminosities used for different selections correspond to those data, for which all elements of the detector essential to each specific analysis were fully functional.

The criteria for the selection of  $WW$  events generally follow those used for the cross-section measurements at  $\sqrt{s} = 161$  and  $172$  GeV, which are described in detail in [1,2]. They are briefly reviewed in section 2. In section 3 the total cross-section and the branching fractions of the  $W$  boson are presented. The determination of the  $W$  mass from the cross-section measurements at all three centre-of-mass energies is given in section 4. The cross-sections at 161 and 172 GeV have been updated after a revision of the luminosity measurements.

The cross-sections determined in this analysis correspond to  $W$  pair production through the three doubly resonant tree-level diagrams (“CC03 diagrams” [3]) involving  $s$ -channel  $\gamma$  and  $Z$  exchange and  $t$ -channel  $\nu$  exchange. The selection efficiencies were defined with respect to these diagrams only and were determined using the full simulation program DELSIM [4,5] with the PYTHIA 5.7 event generator [6]. Depending on the decay mode of each  $W$ , fully hadronic, mixed hadronic-leptonic (“semileptonic”) or fully leptonic final states are obtained. The Standard Model branching fractions are 45.9%, 43.7% and 10.4%, respectively. In addition to their production via the CC03 diagrams, the four-fermion final states corresponding to these decay modes may be produced via other diagrams involving either zero, one, or two massive vector bosons. Corrections which account for the interference between the CC03 diagrams and the additional diagrams are generally expected to be negligible at this energy, except for final states with electrons or positrons. In these cases correction factors were determined from simulation using the 4-fermion generator EXCALIBUR [7] and were found to be consistent with unity within the statistical precision of  $\pm 2\%$ .

## 2 Event selection and cross-sections

### 2.1 Fully hadronic final state

The event selection criteria were optimized in order to ensure that the final state was purely hadronic and in order to reduce the background, dominated by electron-positron annihilation into  $q\bar{q}(\gamma)$ .

For each event, all particles were clustered into jets using the LUCLUS algorithm [8] with  $d_{\text{join}} = 5.5 \text{ GeV}/c$ . At least 4 jets were required, with at least four particles in each jet. Events coming from the radiative return to the  $Z$  peak were rejected by requiring  $\sqrt{s'} > 120 \text{ GeV}$ , where  $\sqrt{s'}$  is an estimate of the effective collision energy after initial state radiation [9].

Events were then forced into a 4-jet configuration, and a kinematically constrained fit performed, imposing energy and momentum conservation. For the separation of  $WW$  events from  $q\bar{q}(\gamma)$  events the variable  $D$  was used:

$$D = \frac{E_{\text{min}}}{E_{\text{max}}} \cdot \frac{\theta_{\text{min}}}{(E_{\text{max}} - E_{\text{min}})}, \quad (1)$$

where  $E_{\min}, E_{\max}$  are the minimum and maximum jet energies and  $\theta_{\min}$  is the smallest interjet angle after the constrained fit. Figure 1 shows the distribution of this quantity after the other cuts described above have been applied.

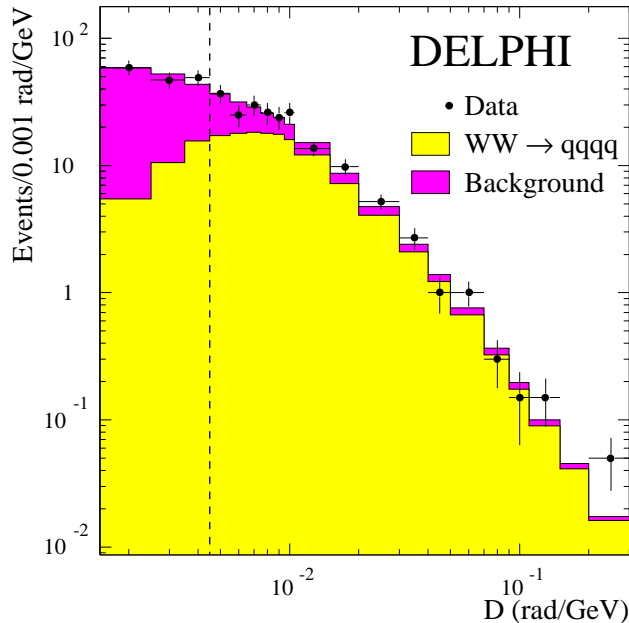


Figure 1: Distribution of the  $D$  variable for 4-jet events. The points show the data and the histograms are the predicted distributions for signal and background. The latter includes small contributions from other  $WW$  channels.

Events were selected with  $D > 0.0045$  rad/GeV and divided into three intervals of  $D$ . For each interval the fractional efficiencies of the selection of  $WW$  decays were estimated from simulation and are listed in table 1. The overall selection efficiency was  $(82.2 \pm 0.8)\%$ . The uncertainty on the efficiency was estimated by comparing real data (taken in 1997 at a centre-of-mass energy of 91.2 GeV) with simulation. For this comparison, the technique of mixing Lorentz-boosted  $Z$  events was used, which transformed two independent hadronic  $Z$  decays into a pseudo  $W$  pair event by applying an appropriate boost to the particles of each  $Z$  decay. In addition, the variation of the efficiency using different hadronization models (JETSET 7.4 [6] and ARIADNE [10]) has been studied and taken into account.

The cross-section for the expected total background was estimated from simulation with the PYTHIA 5.7 event generator [6] to be  $(1.82 \pm 0.08)$  pb. The main contribution comes from  $q\bar{q}(\gamma)$  events with gluon radiation. The systematic uncertainty on the background was estimated from the variation of the selection efficiency for the  $q\bar{q}(\gamma)$  background using generators with different hadronization models [6,10]. Furthermore, the accuracy of the simulation was checked on multihadronic events collected at the  $Z$  pole. These data were selected assuming the 183 GeV criteria downscaled in proportion to the centre-of-mass energy; good agreement was found with the expected numbers of events.

A total of 408 events was selected in the data sample. The cross-section for fully hadronic events was obtained from a binned maximum likelihood fit to the distribution of the variable  $D$ , taking into account the expected background in each bin. The result is

$$\sigma_{WW}^{qqq} = \sigma_{WW}^{tot} \times \text{BR}(WW \rightarrow q\bar{q}q\bar{q}) = 7.19 \pm 0.46 \text{ (stat)} \pm 0.13 \text{ (syst)} \text{ pb},$$

where  $\text{BR}(WW \rightarrow q\bar{q}q\bar{q})$  is the probability for the  $WW$  pair to give a purely hadronic final state, the first error is statistical and the second is systematic. The dominant contribution to the systematic error ( $\pm 0.10$  pb) comes from the uncertainty on the background. The other components are due to uncertainties in the efficiency and luminosity.

channel	efficiencies for selected channels					
	$j\bar{j}j\bar{j}$			$j\bar{j}e\nu$	$j\bar{j}\mu\nu$	$j\bar{j}\tau\nu$
	$D$ interval [ $10^{-3}$ (rad/GeV)]					
	4.5-9.5	9.5-19.0	> 19.0			
$q\bar{q}q\bar{q}$	0.243	0.274	0.305	0.	0.001	0.009
$q\bar{q}e\nu$	0.005	0.002	0.002	0.692	0.001	0.064
$q\bar{q}\mu\nu$	0.003	0.001	0.001	0.003	0.868	0.036
$q\bar{q}\tau\nu$	0.014	0.008	0.005	0.034	0.032	0.428
background (pb)	1.057	0.453	0.305	0.175	0.069	0.410
selected events	142	129	137	92	118	93
luminosity ( $\text{pb}^{-1}$ )	52.52			51.63		52.52

Table 1: Data for the cross-section measurement of the hadronic and semileptonic final states.

## 2.2 Semileptonic final state

Events in which one  $W$  boson decays into a lepton and neutrino and the other into quarks are characterized by two hadronic jets, one isolated lepton (coming either from  $W$  direct decay or from the cascade decay  $W \rightarrow \tau\nu \rightarrow e\nu\nu\nu$  or  $\mu\nu\nu\nu$ ) or a low multiplicity jet due to  $\tau$  decay, and missing momentum resulting from the neutrino(s). The major background comes from  $q\bar{q}(\gamma)$  production and from four-fermion final states containing two quarks and two leptons of the same flavour.

Events were required to have hadronic activity (at least 6 charged particles), a total visible energy of at least 50 GeV and could be described by a 3-jet topology on application of the LUCCLUS algorithm [8] with a value of  $d_{join}$  between 2 and 20 GeV/ $c$ . One of the jets had to be a leptonic jet, according to one of the following criteria:

- The jet consists of a single particle, identified as an electron or muon with an energy of at least 5 GeV.
- The jet consists of a single charged particle, not identified as a lepton, but isolated from other particles (energy above 5 GeV and  $p \cdot \theta_{iso} > 50$  GeV/ $c$ ·degrees, where  $\theta_{iso}$  is the angle to the closest charged particle with a momentum of at least 1 GeV/ $c$ ).
- The jet is of low multiplicity (less than 6 particles in all, and less than 4 charged particles) with an energy between 10 and 60 GeV. The fraction of the charged energy of the candidate  $\tau$  jet with respect to its total energy was required to exceed 15%.

Events with a 2-jet topology and leptons close to fragmentation products or inside a hadronic jet were recovered by looking for particles inside jets with energy above 30 GeV and identified as leptons (electrons or muons). In this case additional criteria were required for the impact parameter of the lepton to the beam spot and for the angles between

the direction of the missing momentum and the beam direction and the direction of the candidate lepton.

The background contribution arising from the radiative return to the  $Z$  peak was reduced by rejecting events with a detected photon of energy above 50 GeV or with the direction of the missing momentum close to the beam axis. The four-fermion neutral current background ( $q\bar{q}\ell\bar{\ell}$ ) was suppressed by applying an additional selection to events in which a second lepton of the same flavour and with charge opposite to that of the main candidate was found. Non-resonant contributions to the  $q\bar{q}\ell\nu$  final state were reduced by requiring the invariant mass of the jet-jet system to be larger than 20 GeV/ $c^2$  and of the lepton - missing momentum system to be larger than 10 GeV/ $c^2$ .

The classification of the different leptonic decays was performed in the following way:

- $WW \rightarrow q\bar{q}\mu\nu$   
The lepton was identified as a muon. The contribution from  $q\bar{q}\tau\nu \rightarrow q\bar{q}\mu\nu\nu\nu$  was suppressed by requiring that, if the muon momentum was lower than 45 GeV/ $c$ , the missing mass in the event was lower than 55 GeV/ $c^2$  or the fitted mass from a 2-constraint kinematic fit with both  $W$ s constrained to have the same mass be greater than 75 GeV/ $c^2$ .
- $WW \rightarrow q\bar{q}e\nu$   
The lepton was identified as an electron. A cut on the acoplanarity of the event, defined as the angle between the lepton direction and the plane of the two jets, was applied in order to reduce radiative and non-radiative QCD background. The contribution from the process  $e^+e^- \rightarrow Ze^+e^-$  was reduced by imposing requirements on the invariant mass of the electron and the missing momentum (assumed to be a single electron in the beam pipe). A procedure identical to that described for the muon channel was then applied to reduce the contamination of  $q\bar{q}\tau\nu$  events in the selected electron sample.
- $WW \rightarrow q\bar{q}\tau\nu$   
The event was not classified as an electron or muon decay. In order to suppress the background from  $e^+e^-$  annihilation into  $q\bar{q}(\gamma)$ , events containing 1-prong jets with momentum lower than 20 GeV/ $c$  were required to have acoplanarity exceeding 25° and the isolation angle of the track had to be greater than 30°. For multi-prong  $\tau$  events a cut on the effective centre-of-mass energy [9] was added, requiring it to be between 100 and 170 GeV.

Figure 2 shows the distribution of the momentum of the selected leptons together with the expectations from simulation of signal and background. The numbers of selected events, efficiencies and backgrounds for each lepton flavour are shown in table 1. The overall efficiency of the selection of  $WW \rightarrow q\bar{q}\ell\nu$  events was estimated to be  $(71.9 \pm 1.3)\%$ , but the efficiencies for selection of the different lepton types varied substantially: 91% for  $\mu$ , 76% for  $e$  and 49% for  $\tau$ . A correction to the efficiency of -1.0% was included to account for the difference in track reconstruction efficiency between data and simulated events and the same amount was added in quadrature to the total systematic error. An uncertainty of  $\pm 1.0\%$  was estimated for an imperfect simulation of the misidentification of electrons or muons as tau leptons from studies of lepton pairs produced at the centre-of mass energy of the  $Z$  boson. The total expected background was estimated to be  $(0.654 \pm 0.053)$  pb. The errors on efficiency and background include all systematic uncertainties.

A total of 303 events was selected as semileptonic  $W$  decays. With the values given in table 1 for selected events, efficiencies and backgrounds, and assuming lepton universality

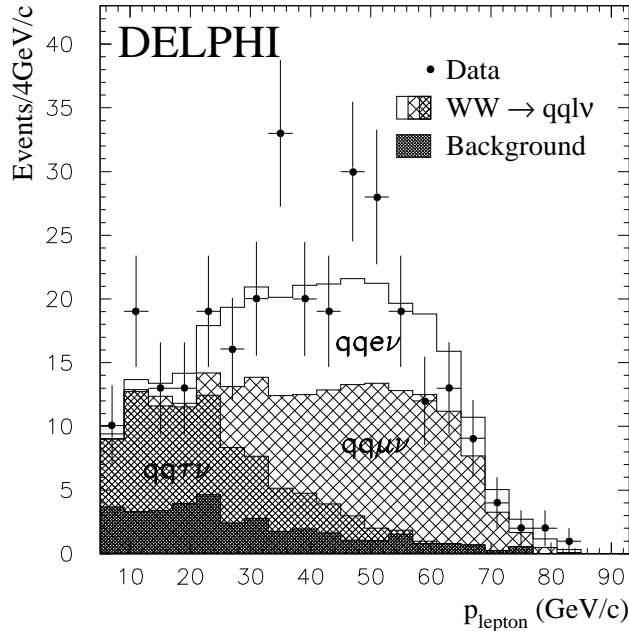


Figure 2: Distribution of the lepton momentum for semileptonic events. The points show the data and the histograms are the predicted distributions for signal and background. The latter includes small contributions from other  $WW$  channels.

a likelihood fit yields a cross-section

$$\sigma_{WW}^{qq\ell\nu} = \sigma_{WW}^{tot} \times \text{BR}(WW \rightarrow q\bar{q}\ell\nu) = 7.11 \pm 0.46 \text{ (stat)} \pm 0.16 \text{ (syst)} \text{ pb.}$$

The systematic error includes contributions from efficiency and background determination, the CC03 correction and from the measurement of the luminosity.

### 2.3 Fully leptonic final state

For the fully leptonic channel ( $WW \rightarrow \ell\nu\ell\nu$ ) low multiplicity events with a clean 2-jet topology were selected. The relevant backgrounds are dileptons from  $e^+e^- \rightarrow Z\gamma$ , Bhabha scattering and two-photon collisions. The selection criteria were similar to those used in [2]; the value of some cuts were rescaled according to the increased centre-of-mass energy.

In the preselection, a charged particle multiplicity between 2 and 5 was required and an acollinearity between the two particles with the highest momenta in the range  $10^\circ < \theta_{acol} < 160^\circ$ . The highest momentum had to be smaller than 80 GeV/c. All particles in the event were clustered into jets using the LUCLUS [8] algorithm with  $d_{join} = 6.5$  GeV/c. Only events with two reconstructed jets, each containing at least one charged particle and either with momentum above 5 GeV/c or associated electromagnetic energy larger than 10 GeV, were retained.

Events from radiative  $Z$  production with the ISR photon entering the detector acceptance were explicitly rejected, requiring that no neutral energy larger than 10 GeV was found in a cone with an aperture of  $10^\circ$  around the beam direction or larger than 50 GeV elsewhere.



To reduce background from  $\gamma\gamma \rightarrow \ell\ell$  events and radiative dilepton events, a selection criterion was applied on the angle  $\theta_{\text{miss}}$  between the direction of the missing momentum and the beam direction. The quantity  $|\cos(\theta_{\text{miss}})|$  was required to be smaller than 0.98, 0.94 and 0.90 according to the event topology assignment a), b) or c), described in the following. In addition, the transverse component of the jet momenta with respect to the two-dimensional thrust axis (which was constructed from the projection of the jet momenta onto the plane transverse to the beam direction) was required to exceed  $2 \text{ GeV}/c$ .

No further cuts were applied to events when there was either (a) one charged particle with at least  $20 \text{ GeV}$  of associated electromagnetic energy and one charged particle with momentum larger than  $5 \text{ GeV}/c$  and identified as a muon, or (b) only one charged particle with momentum larger than  $20 \text{ GeV}/c$  identified as muon and a second jet with a momentum above  $10 \text{ GeV}/c$ .

The remaining events (c) were selected if the momentum of the leading jet was larger than  $25 \text{ GeV}/c$ , that of the other jet between  $5$  and  $70 \text{ GeV}/c$ , the total momentum in the plane transverse to the beam direction larger than  $8 \text{ GeV}/c$  and the total energy in a cone with an aperture of  $20^\circ$  around the beam direction smaller than  $40 \text{ GeV}$ . The energy in the electromagnetic calorimeters was required to be less than  $130 \text{ GeV}$  in total, and less than  $80 \text{ GeV}$  for a single particle.

The leptonic jets were classified as follows:

- $W \rightarrow \mu\nu$   
The jet contained a charged particle identified as muon with momentum larger than  $20 \text{ GeV}/c$ .
- $W \rightarrow e\nu$   
The jet contained either a charged particle with an associated energy in the electromagnetic calorimeters larger than  $20 \text{ GeV}$ , or a charged particle with momentum larger than  $40 \text{ GeV}/c$ , not classified as muon, pointing outside the acceptance of the calorimeters ( $36^\circ < \theta < 42^\circ$ ,  $88^\circ < \theta < 92^\circ$ ,  $138^\circ < \theta < 144^\circ$ ).
- $W \rightarrow \tau\nu$   
The jet was not classified as muon or electron.

The numbers of selected events, efficiencies and backgrounds in each channel are shown in table 2. The overall efficiency for a flavour-blind selection was  $(57.1 \pm 2.1)\%$ . A correction of  $-2.0\%$  was included to account for the difference in the track reconstruction efficiency between data and simulated events and the same amount was added in quadrature to the total systematic error. For misidentification of the lepton type the same uncertainty as in the semileptonic case ( $\pm 1.0\%$ ) was assumed. The residual background from non- $W$  and single- $W$  events is  $0.244 \pm 0.025 \text{ pb}$ .

A total of 59 events was selected in the data sample. With the values given in table 2 for selected events, efficiencies and backgrounds, and assuming lepton universality a likelihood fit yields a cross-section

$$\sigma_{WW}^{\ell\nu\ell\nu} = \sigma_{WW}^{\text{tot}} \times \text{BR}(WW \rightarrow \ell\nu\ell\nu) = 1.54 \pm 0.26 \text{ (stat)} \pm 0.07 \text{ (syst)} \text{ pb.}$$

The systematic error has contributions from the efficiency and background determination, the CC03 correction and from the measurement of the luminosity.

channel	efficiencies for selected channels					
	$e\nu e\nu$	$\mu\nu\mu\nu$	$\tau\nu\tau\nu$	$e\nu\mu\nu$	$e\nu\tau\nu$	$\mu\nu\tau\nu$
$e\nu e\nu$	0.394	0.	0.008	0.008	0.096	0.002
$\mu\nu\mu\nu$	0.	0.600	0.	0.006	0.	0.045
$\tau\nu\tau\nu$	0.002	0.002	0.179	0.006	0.052	0.069
$e\nu\mu\nu$	0.001	0.008	0.001	0.601	0.008	0.085
$e\nu\tau\nu$	0.039	0.	0.050	0.055	0.379	0.009
$\mu\nu\tau\nu$	0.	0.050	0.015	0.053	0.004	0.474
background (pb)	0.045	0.027	0.028	0.034	0.075	0.035
selected events	9	14	4	9	13	10
luminosity ( $\text{pb}^{-1}$ )	51.63					

Table 2: Data for the cross-section measurement of the fully leptonic final state.

### 3 Determination of total cross-section and branching fractions

The total cross-section for  $WW$  production and the  $W$  leptonic branching fractions were obtained from a likelihood fit based on the probabilities of finding the observed number of events in each final state. The input numbers are those given in tables 1 and 2.

From all the final states combined, the branching fractions with their correlation matrix were obtained as shown in table 3. They are consistent with lepton universality. The fit was repeated, assuming lepton universality and the results for the leptonic and derived hadronic branching fraction are also given in table 3. The hadronic branching fraction is in agreement with the Standard Model prediction of 0.677.

channel	branching fraction	stat. error	syst. error	syst. from QCD bkg
$W \rightarrow e\nu$	0.1006	0.0112	0.0028	0.0007
$W \rightarrow \mu\nu$	0.1144	0.0102	0.0023	0.0008
$W \rightarrow \tau\nu$	0.1064	0.0156	0.0041	0.0006
Correlations		$W \rightarrow e\nu$	$W \rightarrow \mu\nu$	$W \rightarrow \tau\nu$
$W \rightarrow e\nu$	1.000	-0.030	-0.332	
$W \rightarrow \mu\nu$	-0.030	1.000	-0.285	
$W \rightarrow \tau\nu$	-0.332	-0.285	1.000	

assuming lepton universality				
channel	branching fraction	stat. error	syst. error	syst. from QCD bkg
$W \rightarrow \ell\nu$	0.1076	0.0052	0.0017	0.0007
$W \rightarrow \text{hadrons}$	0.6771	0.0155	0.0052	0.0021

Table 3:  $W$  branching fractions from 183 GeV data and correlation matrix for the leptonic branching fractions. The uncertainty from the QCD background (column 5) is included in the systematic error (column 4).

Assuming the parameters of the Standard Model, i.e. elements  $|V_{ud}|$ ,  $|V_{us}|$ ,  $|V_{ub}|$ ,  $|V_{cd}|$  and  $|V_{cb}|$  of the CKM matrix, lepton couplings to  $W$  bosons, and the strong coupling constant  $\alpha_S$ , to be fixed at the values given in [11], the measured hadronic branching fraction can be converted into

$$|V_{cs}| = 0.985 \pm 0.073 \text{ (stat)} \pm 0.025 \text{ (syst)},$$

where uncertainties of the Standard Model parameters are included in the systematic error.

The total cross-section for  $WW$  production, with the assumption of Standard Model values for the branching fractions, was found to be

$$\sigma_{WW}^{tot} = 15.86 \pm 0.69 \text{ (stat)} \pm 0.26 \text{ (syst)} \text{ pb.}$$

The measurement of the branching fractions can be improved by combining this measurement with those at lower centre-of-mass energies [1,2]. These results are summarized in table 4.

channel	branching fraction	stat. error	syst. error	syst. from QCD bkg
$W \rightarrow e\nu$	0.1012	0.0107	0.0028	0.0007
$W \rightarrow \mu\nu$	0.1139	0.0096	0.0023	0.0008
$W \rightarrow \tau\nu$	0.1095	0.0149	0.0041	0.0006

Correlations	$W \rightarrow e\nu$	$W \rightarrow \mu\nu$	$W \rightarrow \tau\nu$
$W \rightarrow e\nu$	1.000	-0.028	-0.371
$W \rightarrow \mu\nu$	-0.028	1.000	-0.305
$W \rightarrow \tau\nu$	-0.371	-0.305	1.000

assuming lepton universality				
channel	branching fraction	stat. error	syst. error	syst. from QCD bkg
$W \rightarrow \ell\nu$	0.1085	0.0048	0.0017	0.0007
$W \rightarrow \text{hadrons}$	0.6746	0.0143	0.0052	0.0021

Table 4:  $W$  branching fractions from the combined 161, 172 and 183 GeV data and correlation matrix for the leptonic branching fractions. The uncertainty from the QCD background (column 5) is included in the systematic error (column 4).

## 4 Determination of the $W$ mass

From the measurements of the total cross-sections at 161, 172 and 183 GeV, the mass of the  $W$  boson can be determined assuming the validity of the cross-section dependence predicted by the Standard Model. The cross-sections measured at 161 and 172 GeV differ slightly from those reported in [1,2], due to a revised determination of the luminosity. The new results are listed in table 5 and shown in figure 3. The agreement with the Standard Model prediction using GENTLE [12] is good. From a fit of the revised cross-sections at 161 and 172 GeV together with the newly measured cross-section at 183 GeV to this prediction the mass of the  $W$  boson was determined to be

$$m_W = 80.49 \pm 0.43(\text{stat}) \pm 0.09(\text{syst}) \pm 0.03(\text{LEP}) \text{ GeV}/c^2,$$

in agreement with the determination obtained by direct reconstruction of the  $W$  mass at 172 GeV, which gave  $m_W = 80.22 \pm 0.41(\text{stat}) \pm 0.04(\text{syst}) \pm 0.05(\text{int}) \pm 0.03(\text{LEP})\text{GeV}/c^2$  [2], where “int” denotes the uncertainty from interconnection effects like colour reconnection and Bose-Einstein interference. The LEP error corresponds to an estimated uncertainty on the beam energy of 30 MeV.

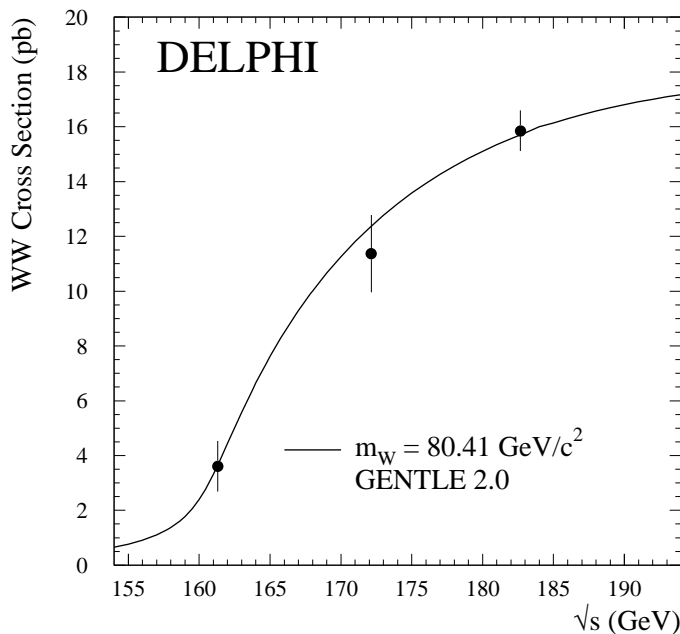


Figure 3: Measurements of the  $W^+W^-$  cross-section compared with the Standard Model prediction using  $m_W = 80.41 \text{ GeV}/c^2$  [11].

Energy (GeV)	luminosity ( $\text{pb}^{-1}$ )	$WW$ cross-section (pb)	stat. error (pb)	syst. error (pb)	syst. from QCD bkg (pb)
161.31	10.07	3.61	0.90	0.19	0.13
172.14	10.12	11.37	1.37	0.32	0.13
182.65	52.52	15.86	0.69	0.26	0.10

Table 5:  $WW$  cross-sections at different centre-of-mass energies. The uncertainty from the QCD background (column 6) is included in the systematic error (column 5).

## 5 Summary

From a data sample of  $53 \text{ pb}^{-1}$  integrated luminosity, collected by DELPHI in  $e^+e^-$  collisions at a centre-of-mass energy of 182.65 GeV, the individual leptonic branching fractions were found to be in agreement with lepton universality and the  $W$  hadronic branching fraction was measured to be

$$\text{BR}(W \rightarrow q\bar{q}) = 0.6771 \pm 0.0155(\text{stat}) \pm 0.0052(\text{syst}).$$

The total cross-section for the doubly resonant process was measured to be

$$\sigma_{WW}^{tot} = 15.86 \pm 0.69(\text{stat}) \pm 0.26(\text{syst}) \text{ pb},$$

assuming Standard Model branching fractions.

The mass of the  $W$  boson determined from the dependence of the cross-section on the centre-of-mass energy has been measured to be:

$$m_W = 80.49 \pm 0.43(\text{stat}) \pm 0.09(\text{syst}) \pm 0.03(\text{LEP}) \text{ GeV}/c^2.$$

## Acknowledgements

We are greatly indebted to our technical collaborators, to the members of the CERN-SL Division for the excellent performance of the LEP collider, and to the funding agencies for their support in building and operating the DELPHI detector.

We acknowledge in particular the support of

Austrian Federal Ministry of Science and Traffics, GZ 616.364/2-III/2a/98,  
FNRS-FWO, Belgium,

FINEP, CNPq, CAPES, FUJB and FAPERJ, Brazil,

Czech Ministry of Industry and Trade, GA CR 202/96/0450 and GA AVCR A1010521,

Danish Natural Research Council,

Commission of the European Communities (DG XII),

Direction des Sciences de la Matière, CEA, France,

Bundesministerium für Bildung, Wissenschaft, Forschung und Technologie, Germany,

General Secretariat for Research and Technology, Greece,

National Science Foundation (NWO) and Foundation for Research on Matter (FOM),

The Netherlands,

Norwegian Research Council,

State Committee for Scientific Research, Poland, 2P03B06015, 2P03B03311 and SPUB/P03/178/98,

JNICT-Junta Nacional de Investigação Científica e Tecnológica, Portugal,

Vedecka grantova agentura MS SR, Slovakia, Nr. 95/5195/134,

Ministry of Science and Technology of the Republic of Slovenia,

CICYT, Spain, AEN96-1661 and AEN96-1681,

The Swedish Natural Science Research Council,

Particle Physics and Astronomy Research Council, UK,

Department of Energy, USA, DE-FG02-94ER40817.

## References

- [1] DELPHI Collaboration, P. Abreu et al., Phys.Lett. **B397** (1997) 158.
- [2] DELPHI Collaboration, P. Abreu et al., E. Phys. J. **C2** (1998) 581.
- [3] W. Beenakker, F. A. Berends et al., *WW Cross-Section and Distributions*, Physics at LEP2, eds. G. Altarelli, T. Sjöstrand and F. Zwirner, CERN 96-01 (1996) Vol 1, 79.
- [4] DELPHI Collaboration: P. Abreu et al., Nucl. Instr. and Meth. **A378** (1996) 57.
- [5] DELPHI Collaboration: *DELPHI event generation and detector simulation - User Guide*, DELPHI Note 89-67 (1989), unpublished.
- [6] T. Sjöstrand, *PYTHIA 5.719 / JETSET 7.4*, Physics at LEP2, eds. G. Altarelli, T. Sjöstrand and F. Zwirner, CERN 96-01 (1996) Vol 2, 41.
- [7] F. A. Berends, R. Kleiss, R. Pittau, *EXCALIBUR*, Physics at LEP2, eds. G. Altarelli, T. Sjöstrand and F. Zwirner, CERN 96-01 (1996) Vol 2, 23.
- [8] T. Sjöstrand, *PYTHIA 5.7 / JETSET 7.4*, CERN-TH.7112/93 (1993).
- [9] P. Abreu et al, *The Estimation of the Effective Centre of Mass Energy in  $q\bar{q}\gamma$  Events from DELPHI*, CERN-OPEN-98-026 (hep-ex/9809008), submitted to Nucl. Instrum. Methods Phys. Res., A.
- [10] L.Lönnblad, Comp.Phys.Comm. **71** (1992) 15.
- [11] Particle Data Group, E. Phys. J. **C3** (1998) 1.
- [12] D. Bardin et al., DESY 95-167 (1995).